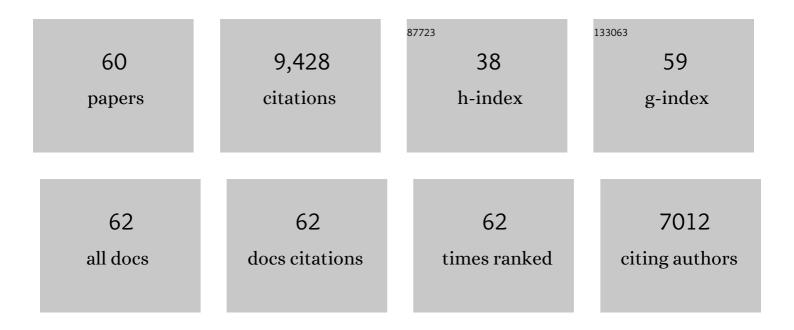


## List of Publications by Year in descending order

Source: https://exaly.com/author-pdf/3333458/publications.pdf Version: 2024-02-01



# ARTICLE IF CITATIONS Dopant-induced electron localization drives CO2 reduction to C2 hydrocarbons. Nature Chemistry, 6.6 2018, 10, 974-980. Molecular tuning of CO2-to-ethylene conversion. Nature, 2020, 577, 509-513. 9 13.7 682 Enhanced Nitrate-to-Ammonia Activity on Copper–Nickel Alloys via Tuning of Intermediate Adsorption. 638 6.6 Journal of the American Chemical Society, 2020, 142, 5702-5708. Steering post-C–C coupling selectivity enables high efficiency electroreduction of carbon dioxide to 4 16.1 537 multi-carbon alcohols. Nature Catalysis, 2018, 1, 421-428. Multi-site electrocatalysts for hydrogen evolution in neutral media by destabilization of water molecules. Nature Energy, 2019, 4, 107-114. 19.8 470 Tuning defects in oxides at roomÂtemperature by lithium reduction. Nature Communications, 2018, 9, 5.8 428 6 1302. Cooperative CO2-to-ethanol conversion via enriched intermediates at molecule–metal catalyst 16.1 390 interfaces. Nature Catalysis, 2020, 3, 75-82. Efficient electrically powered CO2-to-ethanol via suppression of deoxygenation. Nature Energy, 2020, 19.8 8 363 5, 478-486. Copper nanocavities confine intermediates for efficient electrosynthesis of C3 alcohol fuels from 16.1 354 carbon monoxide. Nature Catalysis, 2018, 1, 946-951. Continuous Carbon Dioxide Electroreduction to Concentrated Multi-carbon Products Using a 10 11.7 350 Membrane Electrode Assembly. Joule, 2019, 3, 2777-2791. Binding Site Diversity Promotes CO<sub>2</sub> Electroreduction to Ethanol. Journal of the 338 6.6 American Chemical Society, 2019, 141, 8584-8591. Metalâ€"Organic Frameworks Mediate Cu Coordination for Selective CO<sub>2</sub> 12 6.6 326 Electroreduction. Journal of the American Chemical Society, 2018, 140, 11378-11386. Catalyst synthesis under CO2 electroreduction favours faceting and promotes renewable fuels. 16.1 electrosynthesis. Nature Catalysis, 2020, 3, 98-106. Copper-on-nitride enhances the stable electrosynthesis of multi-carbon products from CO2. Nature 14 5.8 279 Communications, 2018, 9, 3828. Three-dimensional open nano-netcage electrocatalysts for efficient pH-universal overall water 5.8 253 splitting. Nature Communications, 2019, 10, 4875. Coordination engineering of iridium nanocluster bifunctional electrocatalyst for highly efficient 16 5.8 221 and pH-universal overall water splitting. Nature Communications, 2020, 11, 4246. Constraining CO coverage on copper promotes high-efficiency ethylene electroproduction. Nature 16.1 214 Catalysis, 2019, 2, 1124-1131. Hydroxide promotes carbon dioxide electroreduction to ethanol on copper via tuning of adsorbed 18 5.8 201 hydrogen. Nature Communications, 2019, 10, 5814.

Jun Li

#	Article	IF	CITATIONS
19	Efficient Electrocatalytic CO2 Reduction to C2+ Alcohols at Defect-Site-Rich Cu Surface. Joule, 2021, 5, 429-440.	11.7	194
20	Efficient electrocatalytic conversion of carbon monoxide to propanol using fragmented copper. Nature Catalysis, 2019, 2, 251-258.	16.1	188
21	Self-Cleaning CO <sub>2</sub> Reduction Systems: Unsteady Electrochemical Forcing Enables Stability. ACS Energy Letters, 2021, 6, 809-815.	8.8	159
22	Copper adparticle enabled selective electrosynthesis of n-propanol. Nature Communications, 2018, 9, 4614.	5.8	153
23	Efficient upgrading of CO to C3 fuel using asymmetric C-C coupling active sites. Nature Communications, 2019, 10, 5186.	5.8	127
24	Tuning OH binding energy enables selective electrochemical oxidation of ethylene to ethylene glycol. Nature Catalysis, 2020, 3, 14-22.	16.1	120
25	Oxygen-tolerant electroproduction of C <sub>2</sub> products from simulated flue gas. Energy and Environmental Science, 2020, 13, 554-561.	15.6	113
26	Quantum-Dot-Derived Catalysts for CO2 Reduction Reaction. Joule, 2019, 3, 1703-1718.	11.7	106
27	High-Rate and Efficient Ethylene Electrosynthesis Using a Catalyst/Promoter/Transport Layer. ACS Energy Letters, 2020, 5, 2811-2818.	8.8	106
28	Low coordination number copper catalysts for electrochemical CO2 methanation in a membrane electrode assembly. Nature Communications, 2021, 12, 2932.	5.8	97
29	Silica-copper catalyst interfaces enable carbon-carbon coupling towards ethylene electrosynthesis. Nature Communications, 2021, 12, 2808.	5.8	91
30	A high efficiency H <sub>2</sub> S gas sensor material: paper like Fe <sub>2</sub> O <sub>3</sub> /graphene nanosheets and structural alignment dependency of device efficiency. Journal of Materials Chemistry A, 2014, 2, 6714-6717.	5.2	87
31	Enhanced multi-carbon alcohol electroproduction from CO via modulated hydrogen adsorption. Nature Communications, 2020, 11, 3685.	5.8	72
32	Gold-in-copper at low *CO coverage enables efficient electromethanation of CO2. Nature Communications, 2021, 12, 3387.	5.8	70
33	Efficient electrocatalytic conversion of carbon dioxide in a low-resistance pressurized alkaline electrolyzer. Applied Energy, 2020, 261, 114305.	5.1	65
34	Unveiling the In Situ Generation of a Monovalent Fe(I) Site in the Single-Fe-Atom Catalyst for Electrochemical CO <sub>2</sub> Reduction. ACS Catalysis, 2021, 11, 7292-7301.	5.5	51
35	Utilizing the full capacity of carbon black as anode for Na-ion batteries via solvent co-intercalation. Nano Research, 2017, 10, 4378-4387.	5.8	45
36	Controllable CO adsorption determines ethylene and methane productions from CO2 electroreduction. Science Bulletin, 2021, 66, 62-68.	4.3	45

Jun Li

#	Article	IF	CITATIONS
37	Unraveling the Origin of Visible Light Capture by Core–Shell TiO <sub>2</sub> Nanotubes. Chemistry of Materials, 2016, 28, 4467-4475.	3.2	42
38	Mechanical reinforcement fibers produced by gel-spinning of poly-acrylic acid (PAA) and graphene oxide (GO) composites. Nanoscale, 2013, 5, 6265.	2.8	39
39	Tracking the Effect of Sodium Insertion/Extraction in Amorphous and Anatase TiO <sub>2</sub> Nanotubes. Journal of Physical Chemistry C, 2017, 121, 11773-11782.	1.5	28
40	2D XANES–XEOL Spectroscopy Studies of Morphology-Dependent Phase Transformation and Corresponding Luminescence from Hierarchical TiO <sub>2</sub> Nanostructures. Chemistry of Materials, 2015, 27, 3021-3029.	3.2	26
41	Dopant-tuned stabilization of intermediates promotes electrosynthesis of valuable C3 products. Nature Communications, 2019, 10, 4807.	5.8	26
42	Unfolding the Anatase-to-Rutile Phase Transition in TiO <sub>2</sub> Nanotubes Using X-ray Spectroscopy and Spectromicroscopy. Journal of Physical Chemistry C, 2016, 120, 22079-22087.	1.5	23
43	Tracking the Local Effect of Fluorine Self-Doping in Anodic TiO <sub>2</sub> Nanotubes. Journal of Physical Chemistry C, 2016, 120, 4623-4628.	1.5	22
44	Nanoscale Clarification of the Electronic Structure and Optical Properties of TiO <sub>2</sub> Nanowire with an Impurity Phase upon Sodium Intercalation. Journal of Physical Chemistry C, 2015, 119, 17848-17856.	1.5	21
45	Structural and Optical Interplay of Palladium-Modified TiO <sub>2</sub> Nanoheterostructure. Journal of Physical Chemistry C, 2015, 119, 2222-2230.	1.5	18
46	Gold Adparticles on Silver Combine Low Overpotential and High Selectivity in Electrochemical CO <sub>2</sub> Conversion. ACS Applied Energy Materials, 2021, 4, 7504-7512.	2.5	18
47	Revealing the Synergy of Mono/Bimetallic PdPt/TiO2 Heterostructure for Enhanced Photoresponse Performance. Journal of Physical Chemistry C, 2017, 121, 24861-24870.	1.5	16
48	The effect of crystal structure of TiO2 nanotubes on the formation of calcium phosphate coatings during biomimetic deposition. Applied Surface Science, 2017, 396, 1212-1219.	3.1	15
49	Life cycle and economic analysis of chemicals production via electrolytic (bi)carbonate and gaseous CO2 conversion. Applied Energy, 2021, 304, 117768.	5.1	15
50	Facilitating the mechanical properties of a high-performance pH-sensitive membrane by cross-linking graphene oxide and polyacrylic acid. Nanotechnology, 2013, 24, 335704.	1.3	14
51	Molecular Stabilization of Subâ€Nanometer Cu Clusters for Selective CO <sub>2</sub> Electromethanation. ChemSusChem, 2022, 15, .	3.6	11
52	Low temperature amorphous to anatase phase transition of titanium oxide nanotubes. Surface Science, 2019, 680, 68-74.	0.8	9
53	Fingerprint Feature of Atomic Intermixing in Supported AuPd Nanocatalysts Probed by X-ray Absorption Fine Structure. Journal of Physical Chemistry C, 2017, 121, 28385-28394.	1.5	7
54	Comparative life cycle and economic assessments of various value-added chemicals' production <i>&gt;via</i> electrochemical CO <sub>2</sub> reduction. Green Chemistry, 2022, 24, 2927-2936.	4.6	7

Jun Li

#	Article	IF	CITATIONS
55	Near-band-gap luminescence from TiO <sub>2</sub> nanograss–nanotube hierarchical membranes. Canadian Journal of Chemistry, 2015, 93, 106-112.	0.6	6
56	Facile Preparation of TiO2 Nanoclusters on Graphene Templates for Photodegradation of Organic Compounds. Journal of Materials Science and Technology, 2015, 31, 840-844.	5.6	6
57	A simple method to prepare miniature quartz fiber boats with superhydrophobicity. Applied Surface Science, 2012, 258, 2038-2042.	3.1	5
58	Effect of spacing distance on loading capacity and pressure resistance of miniature boat fabricated from superhydrophobic phenylenebenzobisoxazole (PBO) fiber bundles. Colloids and Surfaces A: Physicochemical and Engineering Aspects, 2011, 380, 41-46.	2.3	4
59	Efficient Electroreduction of CO2 in an Ultra-Slim Pressurized Electrolyzer. ECS Meeting Abstracts, 2019, , .	0.0	0
60	Carbon Dioxide Electroreduction to Multi-Carbon Products Using a Large-Scale Membrane Electrode Assembly. ECS Meeting Abstracts, 2019, , .	0.0	0